

Consiglio Nazionale delle Ricerche
Progetto finalizzato «Sistemi
Informatici e Calcolo Parallelo»
Iniziativa di supporto al Calcolo Parallelo

**SUPERCOMPUTING
TOOLS
FOR SCIENCE
AND
ENGINEERING**

a cura di
Domenico Laforenza
e **Raffaele Perego**

FrancoAngeli

A VECTOR AND PARALLEL CODE FOR THE ELASTODYNAMIC EQUATION IN 3-D ANISOTROPIC MEDIA

G. Seriani *, J.M. Carcione **, D. Kosloff ** +
*) Osservatorio Geofisico Sperimentale, Trieste, Italy
+) Hamburg University, Hamburg, West Germany
**) Tel Aviv University, Tel Aviv, Israel

Keywords : parallelization, vectorization, wave propagation, anisotropic elastic media, 3-D wave simulation.

Abstract. This work presents a vectorized and parallelized computer code for solving the equations of dynamic elasticity for a 3-D elastic anisotropic medium. The modeling is based on the rapid expansion method (REM) as time integration algorithm and the Fourier pseudospectral method for the computation of the spatial derivatives. The Fourier method appears very suitable for three-dimensional modeling because it requires a relatively small number of grid points to achieve a specified accuracy. With the REM the time integration is performed with machine accuracy. This modeling scheme was implemented on the CRAY Y-MP/432 with 32 megawords of cpu memory. In order to compute the spatial derivatives and to take advantage of the vectorization properties of the computer, a vector odd-based mixed radix FFT routine was implemented. On the other hand, parallel processing with the four cpu's of the CRAY allows the computation of reasonable geological model within a few hours. An example of 3-D wave propagation in a heterogeneous medium, half anisotropic and half isotropic is shown.

1. Introduction. The problem of wave propagation through anisotropic solids has been extensively developed (Payton, 1983), but exact analytical solutions of the wave field are very difficult to obtain, even in the simplest cases. The equation of motion for solids of low symmetry is extremely complicated. The hexagonal system, which belongs to the class of transversely isotropic solids, is one of the simplest due to the circular symmetry, but analytical solutions are known only along the symmetry axis.

General solutions of the wave field in anisotropic solids can be obtained by solving the equation of motion numerically (Carcione et al., 1988). This is accomplished by using grid methods such as finite elements, finite differences or the Fourier pseudospectral method, which for 3D realistic problems are inefficient when using scalar machines. However, with the recent advances in supercomputer technology, realistic 3D simulations in anisotropic media has become feasible by implementation of the algorithm on multiprocessors computer systems.

The solution of the elastodynamic equations is based on the rapid expansion method (REM) as time integration algorithm and the Fourier method for the computation of the spatial derivatives (Kosloff et al., 1989a). The modeling allows arbitrary elasticities and density in each point of the space. This resolution method allows machine accuracy avoiding the numerical dispersion present in finite differences and finite element methods.

The example shown in this work is solved on a CRAY YMP-432 computer system. Calculations use vectorization and parallel processing architecture, mainly

in the functional operation which computes the spatial derivatives. The first section introduces the basic equations for wave motion in a 3D transversely isotropic elastic solid. Then, the numerical algorithm is briefly described, with emphasis in the costly functional operation previously mentioned. Finally, we present an example of wave propagation in a heterogeneous solid composed of zinc and an isotropic material.

2. Basic equations. The equation of momentum conservation for a 3D elastic medium are (Fung, 1965):

$$\rho \ddot{u}_x = \frac{\partial}{\partial x} \sigma_{xx} + \frac{\partial}{\partial y} \sigma_{xy} + \frac{\partial}{\partial z} \sigma_{xz} + f_x, \quad (1a)$$

$$\rho \ddot{u}_y = \frac{\partial}{\partial x} \sigma_{xy} + \frac{\partial}{\partial y} \sigma_{yy} + \frac{\partial}{\partial z} \sigma_{yz} + f_y, \quad (1b)$$

$$\rho \ddot{u}_z = \frac{\partial}{\partial x} \sigma_{xz} + \frac{\partial}{\partial y} \sigma_{yz} + \frac{\partial}{\partial z} \sigma_{zz} + f_z, \quad (1c)$$

The stress components are σ_{xx} , σ_{yy} , σ_{zz} , σ_{xy} , σ_{yz} and σ_{yz} and f_x , f_y and f_z are the body forces; the displacement components are u_x , u_y and u_z , and ρ denotes the density. A dot above a variable indicates time differentiation.

The constitutive relation for a transversely isotropic solid can be written as

$$\sigma_{xx} = c_{11} \epsilon_{xx} + c_{12} \epsilon_{yy} + c_{13} \epsilon_{zz}, \quad (2a)$$

$$\sigma_{yy} = c_{12} \epsilon_{xx} + c_{11} \epsilon_{yy} + c_{13} \epsilon_{zz}, \quad (2b)$$

$$\sigma_{zz} = c_{13} (\epsilon_{xx} + \epsilon_{yy}) + c_{33} \epsilon_{zz}, \quad (2c)$$

$$\sigma_{xy} = 2c_{66} \epsilon_{xy}, \quad \sigma_{xz} = 2c_{44} \epsilon_{xz}, \quad \sigma_{yz} = 2c_{44} \epsilon_{yz}, \quad (2d)$$

c_{11} , c_{12} , c_{13} , c_{33} and c_{66} are the elasticities with $c_{66} = (c_{11} - c_{12})/2$, and ϵ_{xx} , ϵ_{yy} , ϵ_{zz} , ϵ_{xy} , ϵ_{xz} and ϵ_{yz} are the body strains. In the isotropic limit the elasticities give the Lamé constants:

$$c_{11} \rightarrow c_{33} \rightarrow \lambda + 2\mu, \quad c_{12} \rightarrow c_{13} \rightarrow \lambda, \quad c_{44} \rightarrow c_{66} \rightarrow \mu. \quad (3)$$

Strains can be expressed in terms of displacements as follows:

$$\epsilon_{xx} = \frac{\partial}{\partial x} u_x, \quad \epsilon_{yy} = \frac{\partial}{\partial y} u_y, \quad \epsilon_{zz} = \frac{\partial}{\partial z} u_z, \quad (4a-c)$$

$$\epsilon_{xy} = \frac{1}{2} \left(\frac{\partial}{\partial y} u_x + \frac{\partial}{\partial x} u_y \right), \quad (4d)$$

$$\epsilon_{xz} = \frac{1}{2} \left(\frac{\partial}{\partial x} u_z + \frac{\partial}{\partial z} u_x \right), \quad (4e)$$

$$\epsilon_{yz} = \frac{1}{2} \left(\frac{\partial}{\partial z} u_y + \frac{\partial}{\partial y} u_z \right). \quad (4f)$$

The density ρ and the elasticities are functions of the Cartesian coordinates, while the stresses, strains and displacements depend also on the time variable.

3. Numerical algorithm. The numerical solution is obtained with the rapid expansion method (REM) as time integration technique and the Fourier method for the computation of the spatial derivatives. Replacing the constitutive relations (2a-d) in the equations of momentum conservation (1a-c) and making use of the displacement-strain relations (4a-f), we obtain the equation of motion expressed as

$$\ddot{\mathbf{u}} = -\mathbf{L}^2 \mathbf{u} + \mathbf{f}, \quad (5)$$

where \mathbf{u} is the displacement vector, \mathbf{f} is the body force vector, and $-\mathbf{L}$ is a matrix operator with components

$$-L_{ij}^2 = \frac{1}{\rho} G_{IJ} c_{JK} G_{KJ}^T, \quad i, j = 1, 2, 3 \quad J, K = 1, \dots, 6. \quad (6)$$

with

$$\mathbf{G} = \begin{bmatrix} c_{11} & c_{12} & c_{13} & 0 & 0 & 0 \\ c_{22} & c_{13} & 0 & 0 & 0 & 0 \\ c_{33} & 0 & 0 & 0 & 0 & 0 \\ c_{44} & 0 & 0 & 0 & 0 & 0 \\ c_{44} & 0 & 0 & 0 & 0 & 0 \\ c_{66} & 0 & 0 & 0 & 0 & 0 \end{bmatrix}, \quad \mathbf{G} = \begin{bmatrix} \partial/\partial x & 0 & 0 & 0 & 0 & 0 \\ 0 & \partial/\partial y & 0 & 0 & \partial/\partial z & \partial/\partial y \\ 0 & 0 & \partial/\partial y & 0 & \partial/\partial z & 0 \\ 0 & 0 & \partial/\partial z & \partial/\partial y & \partial/\partial x & 0 \end{bmatrix}, \quad (7)$$

the elasticity matrix and the spatial derivative operator.

The Rapid Expansion Method (REM) solution is

$$\mathbf{u}(t) = \sum_{k \text{ odd}} b_k \mathbf{U}_k \mathbf{g}, \quad (8)$$

for a source term of the type $\mathbf{f} = h(t)\mathbf{g}(\mathbf{x})$, with

$$b_k = \frac{1}{R} \int_0^t J_k(\tau R) h(t - \tau) d\tau, \quad (9)$$

where J_k is the k th-order Bessel function,

$$\mathbf{U}_k = \left[\frac{R}{iL} \right] \mathbf{Q}_k \left[\frac{iL}{R} \right], \quad (10)$$

R is a scalar larger than the range of the eigenvalues of \mathbf{L} and \mathbf{Q}_k are modified Chebyshev polynomials which satisfy the following recursion relation:

$$\mathbf{U}_1 = \mathbf{I}, \quad (11a)$$

$$\mathbf{U}_3 = 3\mathbf{I} - \frac{4L^2}{R^2}, \quad (11b)$$

$$\mathbf{U}_{k+2} = \left[-\frac{4L^2}{R^2} + 2\mathbf{I} \right] \mathbf{U}_k - \mathbf{U}_{k-2} \quad (11c)$$

\mathbf{I} is the identity matrix.

A detailed description of the computational implementation of REM can be found in Kostoff et al., (1989b). Here we are concerned with the most time consuming part of the algorithm which is the functional operation

$$\mathbf{v} = -\mathbf{L}^T \mathbf{u}, \tag{12}$$

where u and v are three-component vectors.

To implement this functional operation into a computer algorithm, the space domain is discretized into a three dimensional array of size $N_x \times N_y \times N_z$, where equation (12) is evaluated. The computation of the spatial derivatives which are involved is done by using the Fast Fourier Transform. In this way the differential operators $\partial/\partial x$, $\partial/\partial y$ and $\partial/\partial z$, are substituted by the operators $\mathbf{d}_l \equiv \mathbf{F}_l^{-1} i K_l \mathbf{F}_l$ (with $l = x, y, z$), where \mathbf{F}_l and \mathbf{F}_l^{-1} represent the direct and inverse Fourier transform operators; K_l is the operator multiplying each Fourier coefficient by its wave number, and $i^2 \equiv -1$. The various steps for calculating the functional operation (12) are summarized schematically in the following steps:

- Compute $\partial u_x/\partial x$, $\partial u_y/\partial x$, $\partial u_z/\partial x$, $\partial u_x/\partial y$, $\partial u_y/\partial y$, $\partial u_z/\partial y$, $\partial u_x/\partial z$, $\partial u_y/\partial z$ and $\partial u_z/\partial z$.
- Compute strains with equations (4a-f).
- Compute stresses with equations (2a-f).
- Compute $\mathbf{v}_x = (\partial \sigma_{xx}/\partial x + \partial \sigma_{xy}/\partial y + \partial \sigma_{xz}/\partial z)/\rho$
- Compute $\mathbf{v}_y = (\partial \sigma_{xy}/\partial x + \partial \sigma_{yy}/\partial y + \partial \sigma_{yz}/\partial z)/\rho$, $\mathbf{v}_z = (\partial \sigma_{xz}/\partial x + \partial \sigma_{yz}/\partial y + \partial \sigma_{zz}/\partial z)/\rho$.

Actually, v_x , v_y and v_z are obtained basically from the calculation of the acceleration $\ddot{\mathbf{u}}$ from the displacements \mathbf{u} as indicated by the equation of motion (5).

From the point of view of storage, the implementation of the REM algorithm needs eighteen arrays for a transversely-isotropic elastic solid, they are:

- Nine arrays of dimension $N_x N_y N_z$ each to store displacement components.
- Six arrays of dimension $N_x N_y N_z$ each to store the material properties, i.e. density and elasticities.
- Three arrays of dimension $N_x N_y N_z$ each to store intermediate results in the computation of the stresses.

4. Implementation and Performance.

The algorithm has been implemented in order to exploit at the maximum the power of modern vector/parallel supercomputers. The computations are dominated by FFT calculations which are highly suited for parallel processing. Moreover, the FFT routine can be efficiently implemented for vector processors (Temperton, 1983) and, in particular, for the Cray X-MP or Y-MP computers.

In practice, let N_x , N_y and N_z denote the number of grid points in the x , y and z directions. Calculation of \mathbf{d}_l^2 (with $l = x, y, z$) are done, for instance, in XY -planes, with multiple FFT's of length N_x or N_y in vector mode. Furthermore, the parallel computing is achieved by allowing each of the available CPUs to operate on separate parallel planes. This scheme is repeated for all parallel planes perpendicular to the two directions (y, z) and it was implemented for a four processor Cray Y-MP using the Autotasking parallelization tool available under Unicos operating system.

Autotasking is performed through a Fortran preprocessor called *ftp* which analyzes the original source code and modifies it introducing vector and parallel directives for the *gft77* compiler. The result is a vectorized and microtasked computing code. In order to produce the parallelization according to the previously discussed scheme, autotasking directives were introduced in the source code. Thus, parallelization was forced only at plane level computations while all other lower level computations were forced in vector mode.

To get the performance of the algorithm, numerical simulations were run in a non dedicated mode. Usually performance tests are run in a dedicated mode but we think that the obtained results are misleading since production jobs normally run in a non dedicated computer environment. The timing data were deducted from the *ja* accounting reports where all the job timing data are reported (user CPU time, total CPUs time, multitasking breakdown, etc.). The average of the concurrent working CPUs is also reported. In order to have statistically valid data, simulations with different storage requirements (1.6, 2.9, 9.4, 14.5 Mw sizes) were repeated many times.

From the *ja* reports it was deduced that the code reaches a very high parallelism, about the 98.8 % of the total computing time is spent in multitasking mode. In pure vector mode, the execution times for a simulation of 1 second and different problem sizes are reported in table 1.

Problem size	125 × 81 × 81	81 × 81 × 81	81 × 45 × 45	45 × 45 × 45
	14.5 Mw	9.4 Mw	2.9 Mw	1.6 Mw
Time	4623.	2881.	992.	663.

Table 1. Performance on the Cray Y-MP in vector mode for different problem sizes. The time is expressed in seconds.

In a non dedicated environment not all the processors are always available at the same time, but they are allocated or taken back to a job according to the overall activity of the other concurrent jobs. For this reason at each run we have to consider not the number of processors but the average of the number of processors that have worked for the job, which is defined as the ratio between the total CPUs time and the total concurrent CPUs connection time.

The speed-up ratio and efficiency (percentage of calculation effort over total CPU effort) versus the average of the concurrent CPUs are shown in Figure 1. It can be seen that they do not correspond to the parallelism level of the code but to a lower parallelism level of the order of 70 %. This can be attributed to the CPU contention, due to the non dedicated environment, and to possible load balancing problems that produce CPU waste time in the waiting on semaphore state. Notice also that the speed-up is not very sensitive to the problem size.

5. Example. The example considers wave propagation in a region consisting of two materials. The upper half-space is zinc and the lower half-space is an isotropic solid. This medium can be considered as an isotropic zinc, since the compressional and shear wave velocities corresponds to the pure longitudinal and pure transverse velocities in zinc (vertical direction). An XZ section of the model is represented in Figure 2. There are no variations in the y direction. Figure 3 displays sections of the wave surfaces for (a) anisotropic zinc, and (b) isotropic zinc. 3D wave surfaces show azimuthal symmetry.

The simulation uses $N_x = 125$, $N_y = 81$ and $N_z = 81$ with $\Delta x = \Delta y = \Delta z = .2 mm$ the grid spacing. The source is located on the interface. Total memory requirements for this example are $18 \times N_x \times N_y \times N_z$, i.e. 15 Mwords. Figure 4 shows snapshots after $t = 25 \mu s$ in several planes containing the source. This is a vertical directional force. The pressure field is calculated as

(12)

$$p = -\frac{1}{3}(\sigma_{xx} + \sigma_{yy} + \sigma_{zz}).$$

Pure pressure waves can propagate in the isotropic medium but not in the anisotropic solid where the qP wave is coupled with the qS wave. This can be appreciated by comparison of the pressure wave field with the u_x component in XZ -planes. In YZ -planes the SH wave can be observed, while XY -planes show isotropic wave propagation.

Acknowledgments

This work was partially supported by grants from the Geophysical Institute of Hamburg University under project 03E-6424-a of the BFMT, West Germany, and project EN3C-0008-D of the Commission of the European Communities. The of us (J.M.C) has been aided by an Alexander Humboldt Scholarship. The numerical simulations were run on the Cray Y-MP of CINECA, Italy, in the frame of Progetto Finalizzato C.N.R. Sistemi Informativi e Calcolo Parallelo.

References

1. Carcione, J. M., Kosloff, D., and Kosloff, R., 1988, *Wave propagation simulation in an elastic anisotropic (transversely isotropic) solid*: Q. JI. Mech. appl. Math., 41, 319-345.
2. Cray Research, 1988, *Autotasking User's Guide*: Technical Report SN-2088, Cray Research, Inc.
3. Kosloff, D., Carcione, J. M., Rommel, B., and Behle, A., 1989a, *Three-dimensional wave propagation simulation in elastic-anisotropic media*: SEG abstracts, 59th Annual Meeting.
4. Kosloff, D., Queiroz Filho, A., Tessmer, E., and Behle, A., 1989b, *Numerical solution of the acoustic and elastic wave equations by a new rapid expansion method*: Geophysical Prospecting, 37, 383-394.
5. Fung, Y. C., 1965, *Foundations of solid mechanics*: Prentice-Hall Inc., Englewood Cliffs, New Jersey.
6. Payton, R. G., 1983, *Elastic wave propagation in transversely isotropic media*: Martinus Nijhoff Publishers.
7. Temperton, C., 1983, *Self-sorting mixed-radix fast Fourier Transform*: J. Comp. Phys., 52, 1-23.

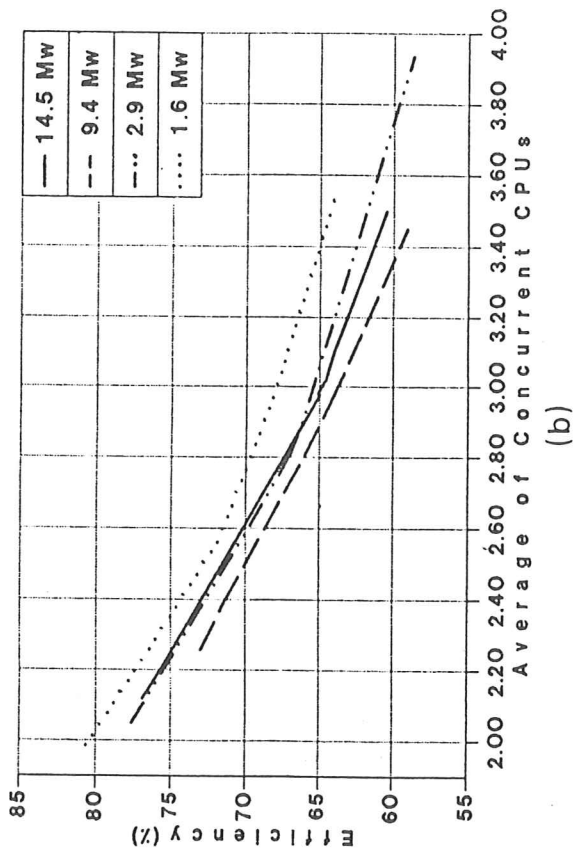
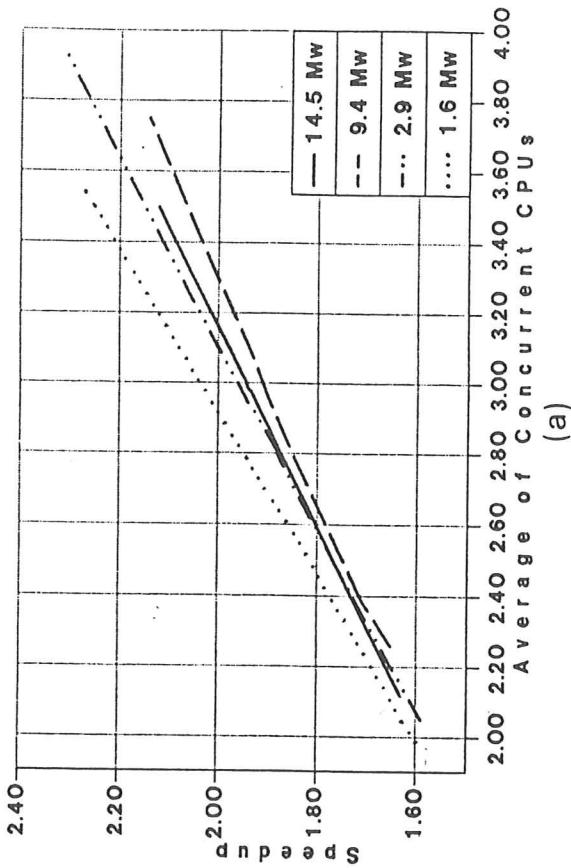


FIG. 1 Speed-up (a) and efficiency (b) versus the average of the number of concurrent CPUs.

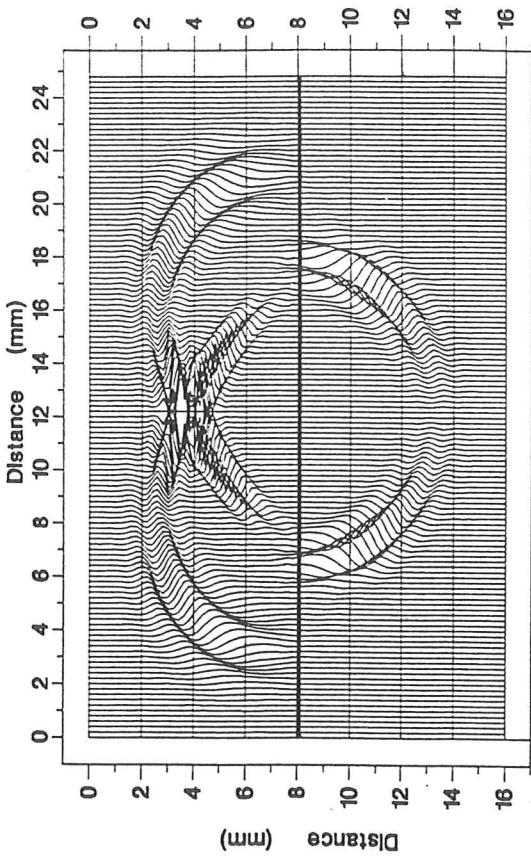


FIG. 2. XZ section of the 3D anisotropic model.

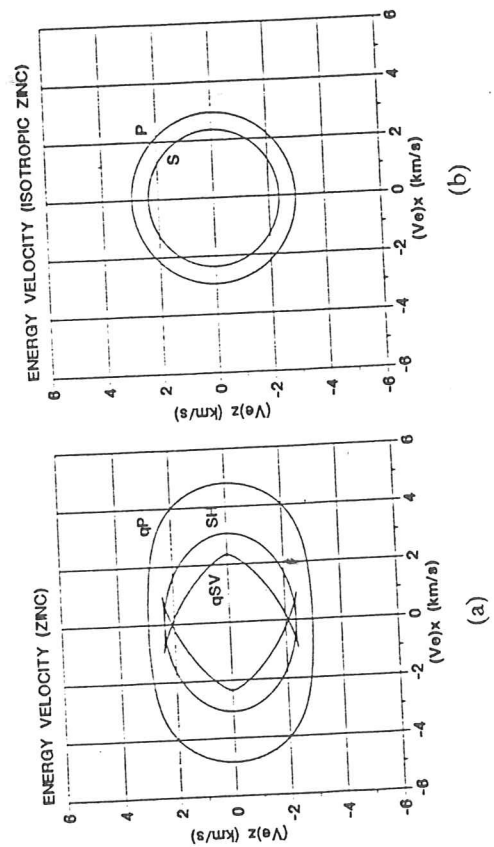
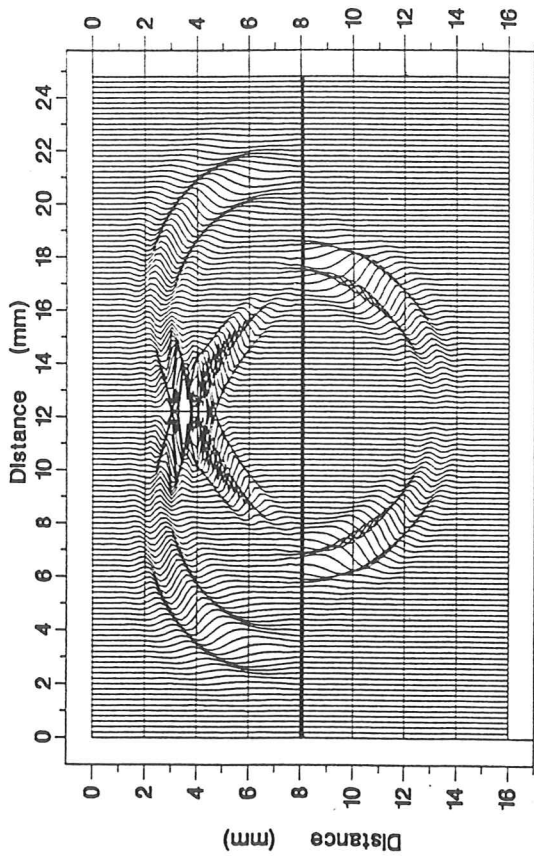
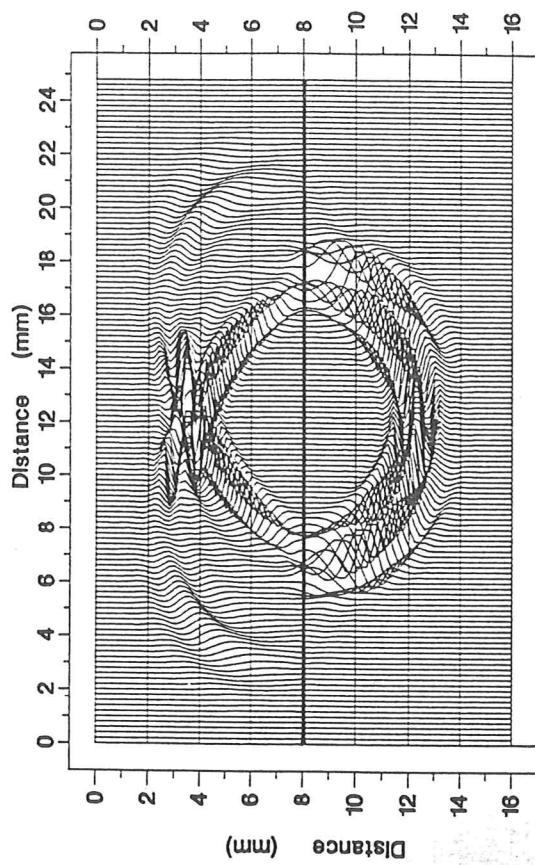


FIG. 3. Sections of the wave surfaces for (a) zinc, and (b) isotropic zinc. 3D wave surfaces show azimuthal symmetry.



Pressure XZ-PLANE



U_x XZ-PLANE

FIG. 4. Snapshots after $t = 25 \mu s$ in several planes containing the source.

Seismic f-k Cascaded Migration: A Parallel Approach

Alessandro Crise, Guido Crispi, Valentina Mosetti
Osservatorio Geofisico Sperimentale, Trieste, Italy

Keywords : seismic, f-k techniques, interactive migration, parallel algorithms, bidimensional FFT

Abstract.

Seismic migration corrects the effects of Earth's response by collapsing the recorded acoustic waves to the originating diffractors. This imaging is obtained by wave field extrapolation methods.

The f-k techniques of migration have been developed in the last ten years to overcome the intrinsic difficulties of finite difference and Kirchhoff methods such as the inability to correctly migrate dipping reflectors.

These f-k methods are very elegant but need to manage the data as a whole, so there are tight constraints in terms of memory allocation and computational power. The implementation of migration on a supercomputer is necessary when real-time results are expected as in the interactive migration.

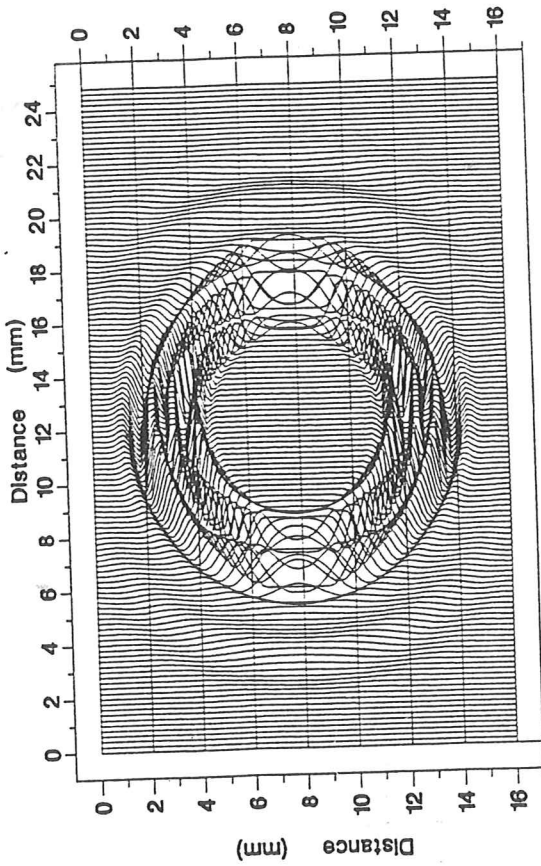
Our implementation makes use of vector and parallel computing facilities available on a CRAY Y-MP supercomputer. Suitable parallel versions of sequential algorithms, e.g. bidimensional FFT and f-k interpolation, were selected and developed. A prototype of cascaded f-k migration was used for testing the effectiveness of the method.

Some results based on real data are reported and future developments are discussed.

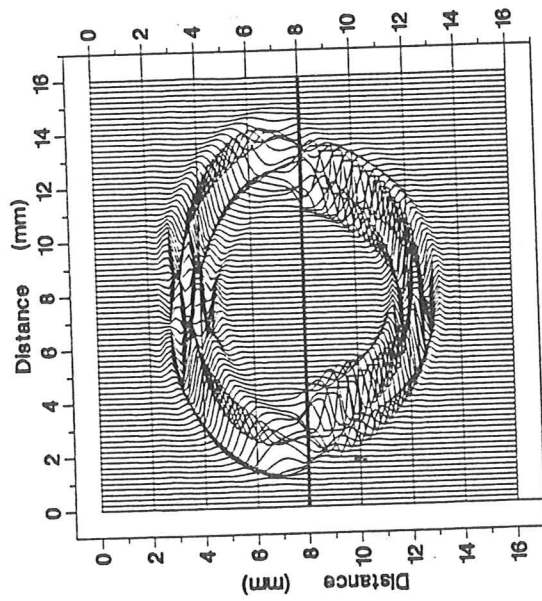
1. Introduction. The study of records of reflected acoustic waves is a powerful instrument for a deeper insight of underground structure. The terrain energization creates a train of waves that are reflected by the seismic horizons and their echoes are recorded at the surface. One of the problems with this kind of data is the mapping of the recorded data at the surface (time-offset section) in a depth-offset section reconstructed at time zero. This imaging is called migration. The migration is a deterministic approach for data inversion, the crucial point for geophysics. Many different algorithms have been proposed to a solution of this problem. One of the most appealing was the migrations in *frequency-wavenumber* (f-k) domain.

2. The f-k and cascaded f-k migration

These methods focus a seismic section by means of a downward continuation of seismic signals recorded at depth $z = 0$. The seismic signal is assumed to be a linear superposition of plane waves. Every plane wave can be shifted back on the generating reflector so as to obtain a concentration of energy on the reflector at time $t = 0$. It is useful to recall some basic definitions and formulae regarding plane waves. It is well known that the Fourier component of a plane wave along



Ux XY-PLANE



Ux YZ-PLANE

FIG. 4 Snapshots after $t = 25 \mu s$ in several planes containing the source.